Introduction of an 8-Aminooctanoic Acid Linker Enhances Uptake of ^{99m}Tc-Labeled Lactam Bridge–Cyclized α-MSH Peptide in Melanoma

Haixun Guo[1], and Yubin Miao[1–3]

[1]College of Pharmacy, University of New Mexico, Albuquerque, New Mexico; [2]Cancer Research and Treatment Center, University of New Mexico, Albuquerque, New Mexico; and [3]Department of Dermatology, University of New Mexico, Albuquerque, New Mexico

The purpose of this study was to examine the effects of amino acid, hydrocarbon, and polyethylene glycol (PEG) linkers on the melanoma targeting and imaging properties of ^{99m}Tc-labeled lactam bridge–cyclized HYNIC-linker-Nle-CycMSH$_{hex}$ (hydrazinonicotinamide-linker-Nle-c[Asp-His-DPhe-Arg-Trp-Lys]-CONH$_2$) peptides. **Methods:** Four novel peptides (HYNIC-GGGNle-CycMSH$_{hex}$, HYNIC-GSGNle-CycMSH$_{hex}$, HYNIC-PEG$_2$Nle-CycMSH$_{hex}$, and HYNIC-AocNle-CycMSH$_{hex}$) were designed and synthesized. The melanocortin-1 receptor binding affinities of the peptides were determined in B16/F1 melanoma cells. The biodistribution of ^{99m}Tc(ethylenediaminediacetic acid [EDDA])-HYNIC-GGGNle-CycMSH$_{hex}$, ^{99m}Tc(EDDA)-HYNIC-GSGNle-CycMSH$_{hex}$, ^{99m}Tc(EDDA)-HYNIC-PEG$_2$Nle-CycMSH$_{hex}$, and ^{99m}Tc(EDDA)-HYNIC-AocNle-CycMSH$_{hex}$ were determined in B16/F1 melanoma–bearing C57 mice at 2 h after injection to select a lead peptide for further evaluation. The melanoma targeting and imaging properties of ^{99m}Tc(EDDA)-HYNIC-AocNle-CycMSH$_{hex}$ were further examined because of its high melanoma uptake. **Results:** The inhibitory concentrations of 50% (IC$_{50}$) for HYNIC-GGGNle-CycMSH$_{hex}$, HYNIC-GSGNle-CycMSH$_{hex}$, HYNIC-PEG$_2$Nle-CycMSH$_{hex}$, and HYNIC-AocNle-CycMSH$_{hex}$ were 0.7 ± 0.1, 0.8 ± 0.09, 0.4 ± 0.08, and 0.3 ± 0.06 nM, respectively, in B16/F1 melanoma cells. Among these four ^{99m}Tc-labeled peptides, ^{99m}Tc(EDDA)-HYNIC-AocNle-CycMSH$_{hex}$ displayed the highest melanoma uptake (22.3 ± 1.72 percentage injected dose/g) at 2 h after injection. ^{99m}Tc(EDDA)-HYNIC-AocNle-CycMSH$_{hex}$ exhibited high tumor–to–normal-organ uptake ratios except for the kidneys. The tumor-to-kidney uptake ratios of ^{99m}Tc(EDDA)-HYNIC-AocNle-CycMSH$_{hex}$ were 3.29, 3.63, and 6.78 at 2, 4, and 24 h, respectively, after injection. The melanoma lesions were clearly visualized by SPECT/CT using ^{99m}Tc(EDDA)-HYNIC-AocNle-CycMSH$_{hex}$ as an imaging probe at 2 h after injection. **Conclusion:** High melanoma uptake and fast urinary clearance of ^{99m}Tc(EDDA)-HYNIC-AocNle-CycMSH$_{hex}$ highlighted its potential for metastatic melanoma detection in the future.

Key Words: alpha-melanocyte-stimulating hormone; ^{99m}Tc-labeled lactam bridge–cyclized peptide; melanoma imaging

Over the past several years, radiolabeled lactam bridge–cyclized α-melanocyte–stimulating hormone (α-MSH) peptides have become another new class of cyclic peptides for melanoma targeting (1–11). The lactam bridge–cyclized α-MSH peptides can bind to the melanocortin-1 (MC1) receptors with low nanomolar binding affinities. Thus, we have used the lactam bridge–cyclized α-MSH peptides to target diagnostic radionuclides (i.e., ^{111}In, ^{67}Ga, and ^{64}Cu) to melanoma cells for imaging. Specifically, we attached DOTA (1,4,7,10-tetraazacyclododecane-1,4,7,10-tetraacetic acid) and NOTA (1,4,7-triazacyclononane-1,4,7-triacetic acid) to the MC1 receptor-targeting GGNle-CycMSH$_{hex}$ (Gly-Gly-Nle-c[Asp-His-DPhe-Arg-Trp-Lys]-CONH$_2$) peptide for radiolabeling of ^{111}In, ^{67}Ga, and ^{64}Cu (9–11). The promising imaging results of ^{111}In-, ^{67}Ga-, and ^{64}Cu-labeled DOTA/NOTA-GGNle-CycMSH$_{hex}$ highlighted their potential as imaging probes for SPECT and PET imaging of melanoma (9–11).

Recently, building on the success of ^{111}In-, ^{67}Ga-, and ^{64}Cu-labeled DOTA/NOTA-GGNle-CycMSH$_{hex}$, we have further developed new ^{99m}Tc-labeled lactam bridge–cyclized α-MSH peptides to take advantage of the ideal imaging properties of ^{99m}Tc (140-keV γ-photon and 6-h half-life) and its wide application in nuclear medicine. Specifically, we replaced DOTA/NOTA with bifunctional metal chelators such as mercaptoacetyltriglycine, Ac-Cys-Gly-Gly-Gly, and hydrazinonicotinamide (HYNIC) for ^{99m}Tc radiolabeling (12). HYNIC-GGNle-CycMSH$_{hex}$ was readily radiolabeled with ^{99m}Tc in ethylenediaminediacetic acid (EDDA)/Tricine solution. Interestingly, ^{99m}Tc(EDDA)-HYNIC-GGNle-CycMSH$_{hex}$ exhibited higher melanoma uptake and faster urinary clearance than ^{99m}Tc-mercaptoacetyltriglycine-GGNle-CycMSH$_{hex}$ and ^{99m}Tc-Ac-Cys-Gly-Gly-Gly-GGNle-CycMSH$_{hex}$ in B16/F1 melanoma–bearing C57 mice. The B16/F1 melanoma lesions were clearly visualized by SPECT/CT using ^{99m}Tc(EDDA)-HYNIC-GGNle-CycMSH$_{hex}$ as an imaging probe (12).

In our previous report, the introduction of the -GlyGly- amino acid linker resulted in lower renal and liver uptake of ^{111}In-DOTA-GGNle-CycMSH$_{hex}$ than of ^{111}In-DOTA-Nle-CycMSH$_{hex}$ (9). Meanwhile, hydrocarbon, amino acid, and polyethylene glycol (PEG) linkers displayed profound favorable effects in the receptor-binding affinities and pharmacokinetics of radiolabeled bombesin (13–17), arginine-glycine-aspartic (18–21), and α-MSH peptides (1,3). Thus, we were interested in examining how the amino acid, hydrocarbon, and PEG linkers affect the melanoma targeting and pharmacokinetic properties of ^{99m}Tc(EDDA)-HYNIC-linker-Nle-CycMSH$_{hex}$ peptides. Building on the HYNIC-GGNle-CycMSH$_{hex}$ construct, we designed in this study 4 novel peptides with different

amino acid, hydrocarbon, and PEG linkers. Two neutral -GlyGlyGly-(GGG) and -GlySerGly- (GSG) amino acid linkers, one -Aoc- (8-aminooctanoic acid) hydrocarbon linker, and one -PEG$_2$- linker were inserted between the HYNIC and Nle-CycMSH$_{hex}$ to generate HYNIC-GGGNle-CycMSH$_{hex}$, HYNIC-GSGNle-CycMSH$_{hex}$, HYNIC-AocNle-CycMSH$_{hex}$, and HYNIC-PEG$_2$Nle-CycMSH$_{hex}$ peptides. The MC1 receptor binding affinities of these 4 peptides were determined in B16/F1 melanoma cells. Then, we radiolabeled the peptides with ^{99m}Tc using the EDDA/Tricine solution. We examined the biodistribution of ^{99m}Tc(EDDA)-HYNIC-GGGNle-CycMSH$_{hex}$, ^{99m}Tc(EDDA)-HYNIC-GSGNle-CycMSH$_{hex}$, ^{99m}Tc(EDDA)-HYNIC-AocNle-CycMSH$_{hex}$, and ^{99m}Tc(EDDA)-HYNIC-PEG$_2$Nle-CycMSH$_{hex}$ at 2 h after injection to select a lead ^{99m}Tc-peptide for further evaluation. ^{99m}Tc(EDDA)-HYNIC-AocNle-CycMSH$_{hex}$ displayed the highest melanoma uptake at 2 h after injection. Therefore, we further determined the biodistribution of ^{99m}Tc(EDDA)-HYNIC-AocNle-CycMSH$_{hex}$ and its property for molecular imaging in B16/F1 melanoma–bearing C57 mice in this study.

MATERIALS AND METHODS

Chemicals and Reagents

Amino acid and resin were purchased from Advanced ChemTech Inc. and Novabiochem. Boc-HYNIC was purchased from VWR International, Inc., for peptide synthesis. ^{125}I-Tyr^2-[Nle^4, D-Phe^7]-α-MSH (^{125}I-Tyr^2-NDP-MSH) was obtained from PerkinElmer, Inc., for the receptor binding assay. ^{99m}TcO$_4^-$ was purchased from Cardinal Health for peptide radiolabeling. All other chemicals used in this study were purchased from Thermo Fischer Scientific and used without further purification. B16/F1 murine melanoma cells were obtained from American Type Culture Collection.

Peptide Synthesis and Receptor Binding Assay

HYNIC-GGGNle-CycMSH$_{hex}$, HYNIC-GSGNle-CycMSH$_{hex}$, HYNIC-AocNle-CycMSH$_{hex}$, and HYNIC-PEG$_2$Nle-CycMSH$_{hex}$ were synthesized using fluorenylmethyloxy carbonyl chemistry, purified by reverse-phase high-performance liquid chromatography (RP-HPLC; Waters), and characterized by liquid chromatography mass spectrometry. Generally, 70 μmol of resin, 210 μmol of each fluorenylmethyloxycarbonyl–protected amino acid, and 210 μmol of Boc-HYNIC were used for the synthesis. Briefly, the intermediate scaffolds of HYNIC(Boc)-[Gly-Gly-Gly/Gly-Ser(Trt)-Gly/Aoc/PEG$_2$]-Nle-Asp(O-2-PhiPr)-His(Trt)-DPhe-Arg(Pbf)-Trp(Boc)-Lys(Dde) were synthesized on H$_2$N-Sieber amide resin by an Advanced ChemTech multiple-peptide synthesizer. The protecting group of Dde was removed by 2% hydrazine for peptide cyclization. The protecting group of 2-phenylisopropyl was removed and the protected peptide was cleaved from the resin by treatment

with a mixture of 2.5% trifluoroacetic acid and 5% triisopropylsilane. Each protected peptide was cyclized by coupling the carboxylic group from the Asp with the ε-amino group from the Lys. The cyclization reaction was achieved by an overnight reaction in dimethylformamide using benzotriazole-1-yl-oxy-tris-pyrrolidino-phosphonium-hexafluorophosphate as a coupling agent in the presence of N,N-diisopropylethylamine. Then, each protected cyclic peptide was dissolved in H$_2$O/CH$_3$CN (50:50) and lyophilized to remove the reagents. The protecting groups were totally removed by treating with a mixture of trifluoroacetic acid, thioanisole, phenol, water, ethanedithiol and triisopropylsilane (87.5:2.5:2.5:2.5:2.5:2.5) for 2 h at room temperature (25°C). Each peptide was precipitated and washed with ice-cold ether 4 times, purified by RP-HPLC, and characterized by liquid chromatography mass spectrometry. The MC1 receptor binding affinities for HYNIC-GGGNle-CycMSH$_{hex}$, HYNIC-GSGNle-CycMSH$_{hex}$, HYNIC-AocNle-CycMSH$_{hex}$, and HYNIC-PEG$_2$Nle-CycMSH$_{hex}$ were determined in B16/F1 melanoma cells by in vitro competitive receptor binding assay according to our published procedure (9).

Peptide Radiolabeling with ^{99m}Tc

^{99m}Tc(EDDA)-HYNIC-GGGNle-CycMSH$_{hex}$, ^{99m}Tc(EDDA)-HYNIC-GSGNle-CycMSH$_{hex}$, ^{99m}Tc(EDDA)-HYNIC-AocNle-CycMSH$_{hex}$, and ^{99m}Tc(EDDA)-HYNIC-PEG$_2$Nle-CycMSH$_{hex}$ were prepared according to our published procedure (12). Briefly, 50 μL of ^{99m}TcO$_4^-$ (37–74 MBq), 10 μL of 1 mg/mL SnCl$_2$ in 0.1N HCl solution, 200 μL of a mixture of 5 mg/mL of EDDA and 25 mg/mL of Tricine aqueous solution, and 10 μL of a 1 mg/mL concentration of each peptide aqueous solution were added to 400 μL of 0.5 M NH$_4$OAc (pH 5.44) in a reaction vial and incubated at 95°C for 30 min. Each radiolabeled peptide was purified to a single species by RP-HPLC on a Vydac C-18 reverse-phase analytic column (Grace) using a 20-min gradient of 20%–30% acetonitrile in 20 mM HCl aqueous solution at a flow rate of 1 mL/min. The purified peptide was purged with N$_2$ gas for 20 min to remove the acetonitrile. The pH of the final solution was adjusted to 5 with 0.1N NaOH and normal saline for animal studies.

Biodistribution Studies

All animal studies were conducted in compliance with Institutional Animal Care and Use Committee approval. In an attempt to select a lead ^{99m}Tc-peptide for further evaluation, the biodistribution of ^{99m}Tc(EDDA)-HYNIC-GGGNle-CycMSH$_{hex}$, ^{99m}Tc(EDDA)-HYNIC-GSGNle-CycMSH$_{hex}$, ^{99m}Tc(EDDA)-HYNIC-AocNle-CycMSH$_{hex}$, and ^{99m}Tc(EDDA)-HYNIC-PEG$_2$Nle-CycMSH$_{hex}$ was examined in B16/F1 melanoma–bearing C57 female mice (Harlan) at 2 h after injection. The C57 mice were subcutaneously inoculated with 1×10^6 B16/F1 cells on the right flank to generate B16/F1 tumors. The weights of tumors reached approximately 0.2 g at 10 d after cell inoculation. Each melanoma-bearing mouse was injected with 0.037 MBq of ^{99m}Tc(EDDA)-HYNIC-GGGNle-CycMSH$_{hex}$,

TABLE 1
IC$_{50}$ Values and Molecular Weights of 4 Peptides

Peptide	IC$_{50}$ (nM)	Calculated MW	Measured MW
HYNIC-GGNle-CycMSH$_{hex}$*	0.6 ± 0.04	1,232.4	1,232.8
HYNIC-GGGNle-CycMSH$_{hex}$	0.7 ± 0.1	1,288.0	1,288.2
HYNIC-GSGNle-CycMSH$_{hex}$	0.8 ± 0.09	1,318.0	1,318.9
HYNIC-PEG$_2$Nle-CycMSH$_{hex}$	0.3 ± 0.06	1,262.0	1,261.8
HYNIC-AocNle-CycMSH$_{hex}$	0.4 ± 0.08	1,257.0	1,257.3

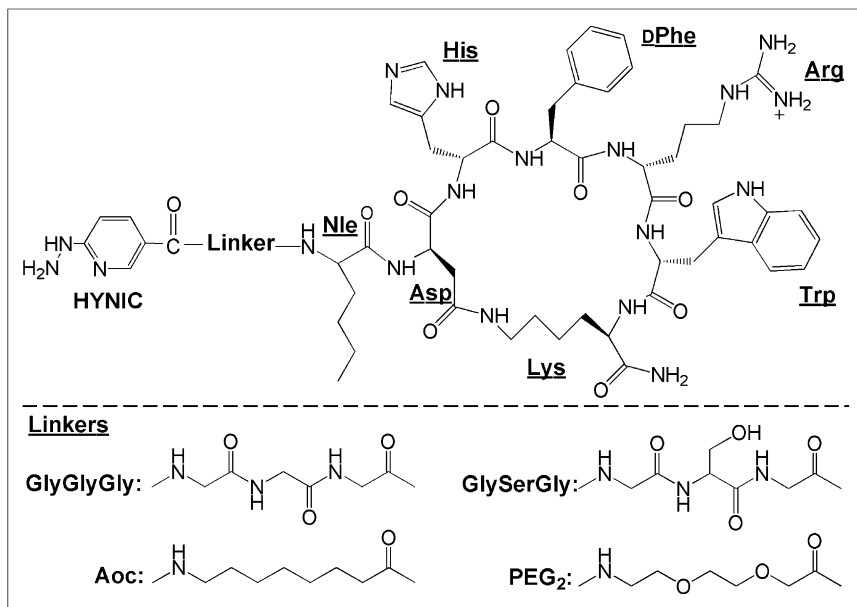*Data are shown for comparison (12).
MW = molecular weight.

FIGURE 1. Schematic structures of HYNIC-linker-Nle-CycMSH$_{hex}$.

^{99m}Tc(EDDA)-HYNIC-GSGNle-CycMSH$_{hex}$, ^{99m}Tc(EDDA)-HYNIC-AocNle-CycMSH$_{hex}$, or ^{99m}Tc(EDDA)-HYNIC-PEG$_2$Nle-CycMSH$_{hex}$ via the tail vein. Groups of 5 mice were sacrificed at 2 h after injection, and tumor and organs of interest were harvested, weighed, and counted in a Wallace 1480 automated γ counter (PerkinElmer). Meanwhile, intestines and urine were collected and counted to evaluate the clearance pathway of each ^{99m}Tc-peptide. Blood was taken as 6.5% of the body weight.

^{99m}Tc(EDDA)-HYNIC-AocNle-CycMSH$_{hex}$ displayed higher melanoma uptake than the other three ^{99m}Tc-peptides. Therefore,
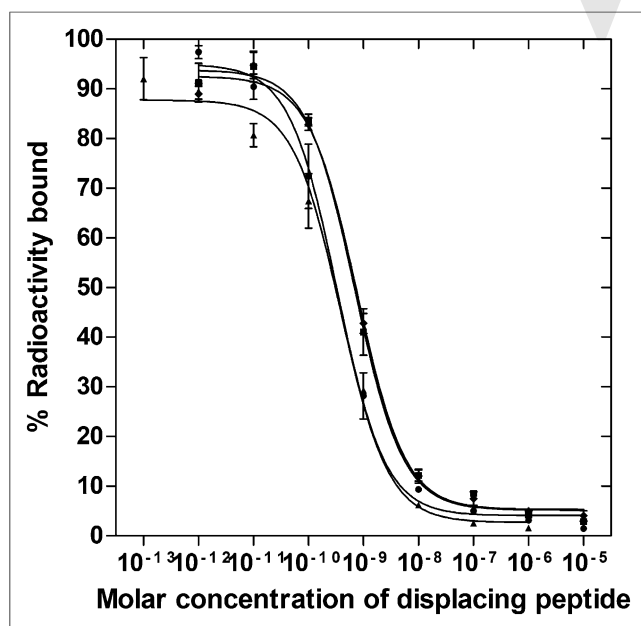

FIGURE 2. In vitro competitive binding curves of HYNIC-PEG$_2$Nle-CycMSH$_{hex}$ (●, IC$_{50}$ = 0.3 ± 0.06 nM), HYNIC-AocNle-CycMSH$_{hex}$ (▲, IC$_{50}$ = 0.4 ± 0.08 nM), HYNIC-GGGNle-CycMSH$_{hex}$ (■, IC$_{50}$ = 0.7 ± 0.1 nM), and HYNIC-GSGNle-CycMSH$_{hex}$ (◆, IC$_{50}$ = 0.8 ± 0.09 nM) in B16/F1 murine melanoma cells.

the biodistribution of ^{99m}Tc(EDDA)-HYNIC-GGNle-CycMSH$_{hex}$ at 0.5, 4, and 24 h after injection was determined in B16/F1 melanoma–bearing C57 female mice. B16/F1 melanoma–bearing mice were generated as described above. Each melanoma-bearing mouse was injected with 0.037 MBq of ^{99m}Tc(EDDA)-HYNIC-AocNle-CycMSH$_{hex}$ via the tail vein. Groups of 5 mice were sacrificed at 0.5, 4, and 24 h after injection, and tumors and organs of interest were harvested, weighed, and counted. Blood was taken as 6.5% of the body weight. The tumor uptake specificity of ^{99m}Tc(EDDA)-HYNIC-AocNle-CycMSH$_{hex}$ was determined by coinjecting 10 μg (6.07 nmol) of unlabeled NDP-MSH peptide at 2 h after injection. To examine whether L-lysine coinjection could decrease the renal uptake, a group of 5 mice was injected with a mixture of 12 mg of L-lysine and 0.037 MBq of ^{99m}Tc(EDDA)-HYNIC-AocNle-CycMSH$_{hex}$. The mice were sacrificed at 2 h after injection, and the tumors and organs of interest were harvested, weighed, and counted.

Melanoma Imaging of ^{99m}Tc(EDDA)-HYNIC-AocNle-CycMSH$_{hex}$

Approximately 9.3 MBq of ^{99m}Tc(EDDA)-HYNIC-AocNle-CycMSH$_{hex}$ were injected in a B16/F1 melanoma–bearing C57 mouse for melanoma imaging. The mouse was euthanized at 2 h after injection for small-animal SPECT/CT (Nano-SPECT/CT; Bioscan) imaging. The 9-min CT imaging was immediately followed by the whole-body SPECT scan. The SPECT scans of 24 projections were acquired. Reconstructed SPECT and CT data were visualized and coregistered using InVivoScope (Bioscan).

Statistical Analysis

Statistical analysis was performed using the Student t test for unpaired data. A 95% confidence level was chosen to determine the significance of differences in tumor and renal uptake of ^{99m}Tc(EDDA)-HYNIC-AocNle-CycMSH$_{hex}$ with and without NDP-MSH coinjection, as well as the significance of differences in tumor and renal uptake of ^{99m}Tc(EDDA)-HYNIC-AocNle-CycMSH$_{hex}$ with and without L-lysine coinjection in the biodistribution studies described above. The differences at the 95% confidence level ($P < 0.05$) were considered significant.

RESULTS

New HYNIC-GGGNle-CycMSH$_{hex}$, HYNIC-GSGNle-CycMSH$_{hex}$, HYNIC-AocNle-CycMSH$_{hex}$, and HYNIC-PEG$_2$Nle-CycMSH$_{hex}$ were synthesized and purified by RP-HPLC. All 4 peptides displayed greater than 95% purity after HPLC purification. The identities of HYNIC-GGGNle-CycMSH$_{hex}$, HYNIC-GSGNle-CycMSH$_{hex}$, HYNIC-AocNle-CycMSH$_{hex}$, and HYNIC-PEG$_2$Nle-CycMSH$_{hex}$ were confirmed by electrospray ionization mass spectrometry. The calculated and found molecular weights of HYNIC-GGGNle-CycMSH$_{hex}$, HYNIC-GSGNle-CycMSH$_{hex}$, HYNIC-AocNle-CycMSH$_{hex}$, and HYNIC-PEG$_2$Nle-CycMSH$_{hex}$ are presented in Table 1. The [Table 1] found molecular weights matched the calculated molecular weights. The schematic structures of HYNIC-GGGNle-CycMSH$_{hex}$, HYNIC-GSGNle-CycMSH$_{hex}$, HYNIC-AocNle-CycMSH$_{hex}$, and HYNIC-PEG$_2$Nle-CycMSH$_{hex}$ are shown in Figure 1. The IC$_{50}$ values of [Fig. 1] HYNIC-GGGNle-CycMSH$_{hex}$, HYNIC-GSGNle-CycMSH$_{hex}$, HYNIC-AocNle-CycMSH$_{hex}$, and HYNIC-PEG$_2$Nle-CycMSH$_{hex}$

TABLE 2
Biodistribution Comparison Among Peptides in B16/F1 Melanoma–Bearing C57 Mice 2 Hours After Injection

Tissue	GGG	GSG	PEG$_2$	Aoc
%ID/g				
Tumor	9.78 ± 3.40	7.41 ± 4.26	14.32 ± 2.82	22.3 ± 1.72
Brain	0.05 ± 0.03	0.07 ± 0.11	0.03 ± 0.02	0.04 ± 0.04
Blood	0.07 ± 0.01	0.08 ± 0.06	0.39 ± 0.07	0.28 ± 0.01
Heart	0.04 ± 0.03	0.06 ± 0.02	0.08 ± 0.03	0.20 ± 0.10
Lung	0.18 ± 0.12	0.15 ± 0.05	0.27 ± 0.12	0.38 ± 0.19
Liver	0.26 ± 0.03	0.23 ± 0.01	0.33 ± 0.03	0.81 ± 0.03
Spleen	0.16 ± 0.09	0.08 ± 0.02	0.11 ± 0.08	0.24 ± 0.00
Stomach	0.43 ± 0.27	0.48 ± 0.39	0.43 ± 0.05	0.70 ± 0.36
Kidneys	5.09 ± 2.19	3.90 ± 1.01	5.79 ± 1.79	6.52 ± 1.04
Muscle	0.03 ± 0.03	0.05 ± 0.02	0.03 ± 0.01	0.06 ± 0.05
Pancreas	0.02 ± 0.01	0.02 ± 0.02	0.08 ± 0.06	0.09 ± 0.00
Bone	0.08 ± 0.06	0.12 ± 0.13	0.29 ± 0.14	0.27 ± 0.10
Skin	0.31 ± 0.10	0.22 ± 0.06	0.49 ± 0.07	0.43 ± 0.11
%ID				
Intestines	0.52 ± 0.09	0.72 ± 0.27	0.99 ± 0.55	1.85 ± 0.51
Urine	93.90 ± 1.47	95.25 ± 0.52	93.19 ± 1.91	88.46 ± 2.23
T/NT				
Liver	37.26	32.26	43.14	27.51
Kidney	1.92	1.90	2.48	3.42
Lung	54.44	50.07	53.72	57.99
Muscle	351.42	146.90	465.25	378.94
Blood	147.62	98.05	36.80	79.79
Skin	31.75	34.01	29.40	52.23

GGG = ^{99m}Tc(EDDA)-HYNIC-GGGNle-CycMSH$_{hex}$; GSG = ^{99m}Tc(EDDA)-HYNIC-GSGNle-CycMSH$_{hex}$; PEG$_2$ = ^{99m}Tc(EDDA)-HYNIC-PEG$_2$Nle-CycMSH$_{hex}$; Aoc = ^{99m}Tc(EDDA)-HYNIC-AocNle-CycMSH$_{hex}$; T/NT = tumor–to–normal-tissue uptake ratio.

Data are %ID/g or %ID (mean ± SD, n = 5).

were 0.7 ± 0.1, 0.8 ± 0.09, 0.4 ± 0.08, and 0.3 ± 0.06 nM in B16/F1 [Fig. 2] melanoma cells, respectively (Fig. 2).

HYNIC-GGGNle-CycMSH$_{hex}$, HYNIC-GSGNle-CycMSH$_{hex}$, HYNIC-AocNle-CycMSH$_{hex}$, and HYNIC-PEG$_2$Nle-CycMSH$_{hex}$ were readily labeled with ^{99m}Tc with greater than 95% radiolabeling yields in EDDA/Tricine solution. Each radiolabeled peptide was completely separated from its excess nonlabeled peptide by RP-HPLC. All ^{99m}Tc-peptides displayed greater than 98% radiochemical purity after HPLC purification. The retention times of ^{99m}Tc(EDDA)-HYNIC-GGGNle-CycMSH$_{hex}$, ^{99m}Tc(EDDA)-HYNIC-GSGNle-CycMSH$_{hex}$, ^{99m}Tc(EDDA)-HYNIC-AocNle-CycMSH$_{hex}$, and ^{99m}Tc(EDDA)-HYNIC-PEG$_2$Nle-CycMSH$_{hex}$ were 12.7, 10.6, 24.0, and 16.8 min, respectively. The retention times of HYNIC-GGGNle-CycMSH$_{hex}$, HYNIC-GSGNle-CycMSH$_{hex}$, HYNIC-AocNle-CycMSH$_{hex}$, and HYNIC-PEG$_2$Nle-CycMSH$_{hex}$ were 9.5, 8.3, 17.9, and 14.6 min, respectively.

The melanoma-targeting and pharmacokinetic properties of ^{99m}Tc(EDDA)-HYNIC-GGGNle-CycMSH$_{hex}$, ^{99m}Tc(EDDA)-HYNIC-GSGNle-CycMSH$_{hex}$, ^{99m}Tc(EDDA)-HYNIC-AocNle-CycMSH$_{hex}$, and ^{99m}Tc(EDDA)-HYNIC-PEG$_2$Nle-CycMSH$_{hex}$ were determined in B16/F1 melanoma–bearing mice at 2 h after injection to select a lead radiolabeled peptide for further evaluation. The biodistri-

bution results of these four ^{99m}Tc-peptides are shown in Table 2. [Table 2] ^{99m}Tc(EDDA)-HYNIC-GGGNle-CycMSH$_{hex}$ and ^{99m}Tc(EDDA)-HYNIC-GSGNle-CycMSH$_{hex}$ displayed substantial tumor uptake of 9.78 ± 3.40 percentage injected dose (%ID)/g and 7.41 ± 4.26 %ID/g at 2 h after injection. ^{99m}Tc(EDDA)-HYNIC-PEG$_2$Nle-CycMSH$_{hex}$ showed higher tumor uptake of 14.32 ± 2.82 %ID/g at 2 h after injection. ^{99m}Tc(EDDA)-HYNIC-AocNle-CycMSH$_{hex}$ exhibited the highest tumor uptake of 22.3 ± 1.72 %ID/g at 2 h after injection among all four ^{99m}Tc-peptides. All ^{99m}Tc-peptides showed fast urinary clearance, approximately 89%–94% of injected activity had cleared the body at 2 h after injection. The accumulation in all normal organs except the kidney was lower than 0.81 %ID/g at 2 h after injection for all four ^{99m}Tc-peptides. The renal uptake values were in a similar range (3.9–6.5 %ID/g at 2 h after injection) for all four ^{99m}Tc-peptides. Thus, we selected ^{99m}Tc(EDDA)-HYNIC-AocNle-CycMSH$_{hex}$ as a lead peptide to further examine its full biodistribution and melanoma-imaging properties.

The full biodistribution results of ^{99m}Tc(EDDA)-HYNIC-AocNle-CycMSH$_{hex}$ are presented in Table 3. ^{99m}Tc(EDDA)-HYNIC- [Table 3] AocNle-CycMSH$_{hex}$ displayed high tumor uptake and prolonged tumor retention in B16/F1 melanoma–bearing C57 mice. The tumor uptake was 23.44 ± 3.37 %ID/g and 22.8 ± 1.71 %ID/g at

TABLE 3
Biodistribution of ^{99m}Tc(EDDA)-HYNIC-AocNle-CycMSH$_{hex}$ in B16/F1 Melanoma–Bearing C57 Mice

Tissue	0.5 h	2 h	4 h	24 h	2-h NDP blockade	2-h L-lys coinjection
%ID/g						
Tumor	23.44 ± 3.37	22.8 ± 1.71	22.17 ± 5.93	7.13 ± 0.99	1.26 ± 0.59*	25.85 ± 6.8
Brain	0.17 ± 0.07	0.05 ± 0.03	0.02 ± 0.02	0.01 ± 0.01	0.03 ± 0.01	0.03 ± 0.01
Blood	2.98 ± 1.77	0.40 ± 0.14	0.30 ± 0.14	0.09 ± 0.03	0.82 ± 0.15	0.18 ± 0.13
Heart	1.75 ± 0.31	0.23 ± 0.08	0.13 ± 0.09	0.07 ± 0.02	0.32 ± 0.09	0.14 ± 0.01
Lung	4.06 ± 1.60	0.52 ± 0.20	0.50 ± 0.19	0.14 ± 0.02	0.91 ± 0.06	0.59 ± 0.06
Liver	3.19 ± 0.39	1.09 ± 0.33	1.26 ± 0.60	0.36 ± 0.01	1.22 ± 0.12	1.22 ± 0.15
Spleen	0.94 ± 0.72	0.30 ± 0.13	0.32 ± 0.13	0.05 ± 0.04	0.17 ± 0.11	0.22 ± 0.09
Stomach	2.52 ± 0.22	1.07 ± 0.10	0.73 ± 0.21	0.11 ± 0.02	0.56 ± 0.10	0.97 ± 0.36
Kidneys	19.65 ± 7.36	6.92 ± 1.40	6.10 ± 0.72	1.05 ± 0.07	6.05 ± 1.13	4.64 ± 0.48*
Muscle	0.43 ± 0.14	0.04 ± 0.03	0.04 ± 0.03	0.02 ± 0.01	0.06 ± 0.05	0.07 ± 0.06
Pancreas	0.97 ± 0.40	0.19 ± 0.14	0.44 ± 0.64	0.06 ± 0.03	0.31 ± 0.10	0.06 ± 0.02
Bone	1.09 ± 0.28	0.15 ± 0.09	0.19 ± 0.15	0.12 ± 0.07	0.30 ± 0.08	0.33 ± 0.30
Skin	3.62 ± 0.35	0.46 ± 0.10	0.37 ± 0.11	0.15 ± 0.05	0.45 ± 0.06	0.54 ± 0.10
%ID						
Intestines	2.43 ± 0.31	1.85 ± 0.51	3.43 ± 0.76	0.32 ± 0.09	1.85 ± 0.42	1.64 ± 0.40
Urine	60.22 ± 4.46	88.46 ± 2.23	84.47 ± 4.80	96.84 ± 1.17	91.29 ± 0.70	88.11 ± 1.90
T/NT						
Liver	7.34	20.86	17.62	20.05	1.03	21.19
Kidney	1.19	3.29	3.63	6.78	0.21	5.57
Lung	5.78	43.77	44.51	52.05	1.39	44.16
Muscle	54.62	527.80	502.79	450.68	21.12	392.26
Blood	7.87	57.59	74.61	82.89	1.54	139.85
Skin	6.47	49.13	59.92	47.99	2.82	47.44

*$P < 0.05$ for differences in tumor and kidney uptake between ^{99m}Tc(EDDA)-HYNIC-AocNle-CycMSH$_{hex}$ with and without peptide blockade, and with and without L-lys coinjection at 2 h after injection.

T/NT = tumor–to–normal-tissue uptake ratio.

Two-hour data are cited from Table 2 for comparison. Data are %ID/g or %ID (mean ± SD, $n = 5$).

0.5 and 2 h after injection, respectively. As compared with the tumor uptake at 2 h after injection, 97.2% of the radioactivity remained in the tumor at 4 h after injection. In the melanoma uptake–blocking study, coinjection of NDP-MSH blocked 94.5% of tumor uptake ($P < 0.05$) at 2 h after injection, demonstrating that the tumor uptake was MC1 receptor-mediated. Normal-organ uptake of ^{99m}Tc(EDDA)-HYNIC-AocNle-CycMSH$_{hex}$ was lower than 1.26 %ID/g in normal tissues except for kidneys at 2, 4, and 24 h after injection. High tumor-to-blood and high tumor–to–normal-organ uptake ratios were achieved as early as 0.5 h after injection. As the major excretion pathway of ^{99m}Tc(EDDA)-HYNIC-AocNle-CycMSH$_{hex}$, the kidney uptake was 19.65 ± 7.36 %ID/g at 0.5 h after injection and decreased to 1.05 ± 0.07 %ID/g at 24 h after injection. The tumor-to-kidney uptake ratios of ^{99m}Tc(EDDA)-HYNIC-AocNle-CycMSH$_{hex}$ were 3.29, 3.63, and 6.78 at 2, 4, and 24 h, respectively, after injection. Coinjection of NDP-MSH did not reduce the renal uptake of the ^{99m}Tc(EDDA)-HYNIC-AocNle-CycMSH$_{hex}$ activity at 2 h after injection, indicating that the renal uptake was not MC1 receptor–mediated. Meanwhile, L-lysine coinjection decreased 33% of the renal uptake ($P < 0.05$) without affecting the tumor uptake. Moreover, ^{99m}Tc(EDDA)-HYNIC-AocNle-CycMSH$_{hex}$ exhibited rapid urinary excretion. Approximately 88% of the activity cleared out of the body at 2 h after injection. The representative whole-body, coronal, and transversal SPECT/CT images are presented in Figure 3. The melanoma lesions were [Fig. 3] clearly visualized by SPECT/CT using ^{99m}Tc(EDDA)-HYNIC-AocNle-CycMSH$_{hex}$ as an imaging probe at 2 h after injection. ^{99m}Tc(EDDA)-HYNIC-AocNle-CycMSH$_{hex}$ exhibited high tumor–to–normal-organ uptake ratios except for the kidneys, which was consistent with the biodistribution results.

DISCUSSION

Over the past several years, a number of research groups have reported ^{99m}Tc-labeled α-MSH peptides (2,5,8,12,22–24) to target the MC1 receptors for melanoma imaging, taking advantage of the ideal imaging properties of ^{99m}Tc. Recently, we have developed a novel class of radiolabeled lactam bridge–cyclized α-MSH peptides to target MC1 receptors for melanoma imaging. Specifically, we have radiolabeled HYNIC/DOTA/NOTA-GGNle-CycMSHhex with ^{99m}Tc, ^{111}In, ^{67}Ga, and ^{64}Cu for SPECT and PET imaging of melanoma (9–12). In our previous report, we found that the Nle-CycMSHhex

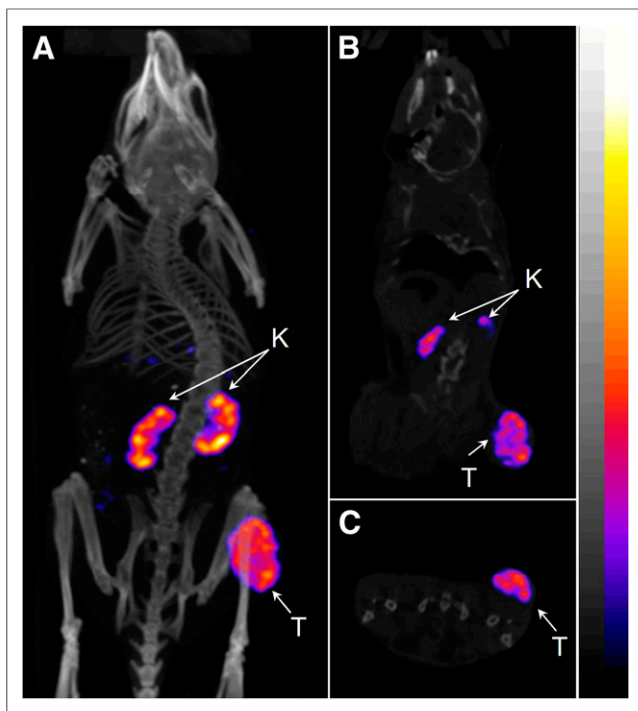**FIGURE 3.** Representative whole-body (A), coronal (B), and transversal (C) SPECT/CT images of ^{99m}Tc(EDDA)-HYNIC-AocNle-CycMSH$_{hex}$ in B16/F1 melanoma–bearing C57 mouse at 2 h after injection. K = kidney; T = tumor.

RGB

FIGURE 4. Comparison of tumor-to-kidney ratios between ^{99m}Tc (EDDA)-HYNIC-GGNle-CycMSH$_{hex}$ and ^{99m}Tc(EDDA)-HYNIC-AocNle-CycMSH$_{hex}$ at 0.5, 2, 4, and 24 h after injection. Data on ^{99m}Tc(EDDA)-HYNIC-GGNle-CycMSH$_{hex}$ (12) are shown for comparison.

moiety was critical for nanomolar MC1 receptor binding affinity of the DOTA-conjugated peptide (9). Introduction of a -GlyGlu-linker between the Nle and CycMSHhex moiety sacrificed the receptor-binding affinity by 485-fold (9). Meanwhile, HYNIC was a better chelator for ^{99m}Tc than other N$_3$S chelators in terms of melanoma uptake and urinary clearance (12). In this study, we managed to examine the effects of amino acid, hydrocarbon, and PEG linkers on the melanoma-targeting properties of ^{99m}Tc-labeled lactam bridge–cyclized α-MSH peptide. Specifically, we introduced -GGG-, -GSG-, -Aoc-, and -PEG$_2$- linkers between the HYNIC and Nle-CycMSHhex moiety to generate new HYNIC-GGGNle-CycMSH$_{hex}$, HYNIC-GSGNle-CycMSH$_{hex}$, HYNIC-AocNle-CycMSH$_{hex}$, and HYNIC-PEG$_2$Nle-CycMSH$_{hex}$ peptides. The lengths of the -GGG-, -GSG-, -Aoc-, and -PEG$_2$- linkers are the same, eliminating the effect of linker length on the melanoma-targeting properties.

The introduction of -GGG-, -GSG-, -Aoc-, and -PEG$_2$- linkers retained the low-nanomolar MC1 receptor binding affinities of the peptides. The IC$_{50}$ was 0.7 ± 0.1 nM for HYNIC-GGGNle-CycMSH$_{hex}$, 0.8 ± 0.09 nM for HYNIC-GGGNle-CycMSH$_{hex}$, 0.4 ± 0.08 nM for HYNIC-AocNle-CycMSH$_{hex}$, and 0.3 ± 0.06 nM for HYNIC-PEG$_2$Nle-CycMSH$_{hex}$ (Table 1), respectively. Furthermore, we radiolabeled these 4 peptides with ^{99m}Tc and determined their biodistribution properties in B16/F1 melanoma–bearing C57 mice at 2 h after injection to examine how the amino acid, hydrocarbon, and PEG linkers affected their melanoma-targeting and pharmacokinetic properties. Despite the slight difference in receptor-binding affinity among HYNIC-GGGNle-CycMSH$_{hex}$, HYNIC-GSGNle-CycMSH$_{hex}$, HYNIC-AocNle-CycMSH$_{hex}$, and HYNIC-PEG$_2$Nle-CycMSH$_{hex}$ peptides, we observed a dramatic difference in melanoma uptake among these four ^{99m}Tc-peptides.
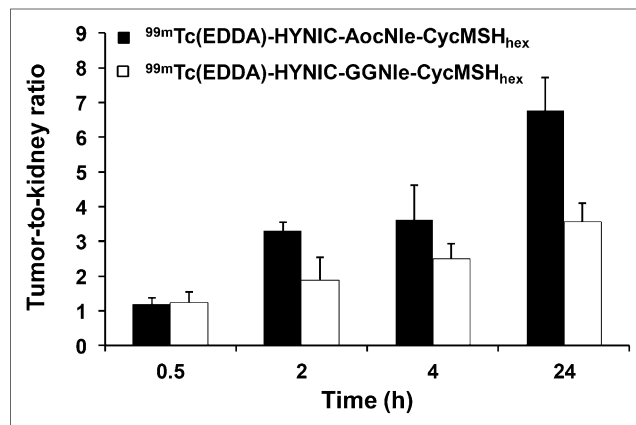
As shown in Table 2, ^{99m}Tc(EDDA)-HYNIC-AcoNle-CycMSH$_{hex}$ exhibited the highest tumor uptake among these four ^{99m}Tc-peptides at 2 h after injection in B16/F1 melanoma–bearing C57 mice. The tumor uptake of ^{99m}Tc(EDDA)-HYNIC-AcoNle-CycMSH$_{hex}$ was 2.3, 3.0, and 1.6 times the tumor uptake of ^{99m}Tc(EDDA)-HYNIC-GGGNle-CycMSH$_{hex}$, ^{99m}Tc(EDDA)-HYNIC-GSGNle-CycMSH$_{hex}$, and ^{99m}Tc(EDDA)-HYNIC-PEG$_2$Nle-CycMSH$_{hex}$, respectively, at 2 h after injection. Thus, we further examined the full biodistribution and melanoma-imaging properties of ^{99m}Tc(EDDA)-HYNIC-AocNle-CycMSH$_{hex}$.

As shown in Table 3, ^{99m}Tc(EDDA)-HYNIC-AocNle-CycMSH$_{hex}$ displayed high tumor uptake and prolonged tumor retention in B16/F1 melanoma–bearing C57 mice. The tumor uptake was 23.44 ± 3.37 %ID/g and 22.8 ± 1.71 %ID/g at 0.5 and 2 h after injection, respectively. In comparison with the tumor uptake at 2 h after injection, 97.2% of the radioactivity remained in tumor at 4 h after injection. Coinjection of NDP-MSH blocked 94.5% of tumor uptake ($P < 0.05$) without affecting the renal uptake at 2 h after injection, demonstrating that the tumor uptake was MC1 receptor–mediated and that renal uptake was nonspecific. ^{99m}Tc(EDDA)-HYNIC-AocNle-CycMSH$_{hex}$ exhibited low accumulation in normal organs and rapid urinary excretion, resulting in high tumor–to–normal-organ uptake ratios. As we anticipated, the B16/F1 melanoma lesions were clearly visualized by SPECT/CT using ^{99m}Tc(EDDA)-HYNIC-AocNle-CycMSH$_{hex}$ as an imaging probe.

Recently, it has been reported that one more carboxylic group resulted in a dramatic decrease in the renal and liver uptake of ^{99m}Tc(CO)$_3$-labeled lactam bridge–cyclized α-MSH peptides (8). Accordingly, we anticipate that the introduction of a negatively charged amino acid would further reduce the renal uptake. In this study, L-lysine coinjection decreased 33% of the renal uptake ($P < 0.05$) without affecting the tumor uptake, indicating that the overall positive charge of ^{99m}Tc(EDDA)-HYNIC-AocNle-CycMSH$_{hex}$ contributed to its nonspecific renal uptake. As shown in Figure 1, there was a positively charged side chain in Arg[8], which contributed to the overall positive charge of ^{99m}Tc(EDDA)-HYNIC-AocNle-CycMSH$_{hex}$. However, the Arg[8] is critical for MC1 receptor binding. Thus, it would be better to introduce a negatively charged amino acid between the HYNIC and Aoc linker to decrease the overall positive charge of the peptide.

In this study, ^{99m}Tc(EDDA)-HYNIC-GGNle-CycMSH$_{hex}$ and ^{99m}Tc-(Arg^{11})CCMSH displayed comparably high melanoma uptake (13.23 ± 2.35 vs. 11.16 ± 1.77 %ID/g) at 4 h after injection. Remarkably, the tumor uptake of ^{99m}Tc(EDDA)-HYNIC-AocNle-CycMSH$_{hex}$ was 1.7 times the tumor uptake of ^{99m}Tc(EDDA)-HYNIC-GGNle-CycMSH$_{hex}$ at 4 h after injection. Meanwhile, ^{99m}Tc(EDDA)-HYNIC-AocNle-CycMSH$_{hex}$ displayed higher tumor-to-kidney uptake ratios than ^{99m}Tc(EDDA)-HYNIC-GGNle-CycMSH$_{hex}$ at 2, 4, and 24 h after injection (Fig. 4). The tumor-to-kidney uptake ratio of ^{99m}Tc(EDDA)-HYNIC-AocNle-CycMSH$_{hex}$ was 1.8, 1.5, and 1.9 times the tumor-to-kidney uptake ratio of ^{99m}Tc(EDDA)-HYNIC-GGNle-CycMSH$_{hex}$ at 2, 4, and 24 h after injection, respectively.

CONCLUSION

The biodistribution of ^{99m}Tc(EDDA)-HYNIC-GGGNle-CycMSH$_{hex}$, ^{99m}Tc(EDDA)-HYNIC-GSGNle-CycMSH$_{hex}$, ^{99m}Tc(EDDA)-HYNIC-AocNle-CycMSH$_{hex}$, and ^{99m}Tc(EDDA)-HYNIC-PEG$_2$Nle-CycMSH$_{hex}$ was determined in B16/F1 melanoma–bearing C57 mice in this study. Among these four ^{99m}Tc-peptides, ^{99m}Tc(EDDA)-HYNIC-AocNle-CycMSH$_{hex}$ exhibited the highest melanoma uptake (22.3 ± 1.72 %ID/g) and tumor-to-kidney uptake ratio at 2 h after injection. Overall, the properties of high melanoma uptake and fast urinary clearance of ^{99m}Tc(EDDA)-HYNIC-AocNle-CycMSH$_{hex}$ highlight its future clinical potential as an imaging probe for metastatic melanoma detection.

DISCLOSURE

ACKNOWLEDGMENTS

REFERENCES

1. Miao Y, Gallazzi F, Guo H, Quinn TP. ^{111}In-labeled lactam bridge-cyclized alpha-melanocyte stimulating hormone peptide analogues for melanoma imaging. *Bioconjug Chem.* 2008;19:539–547.
2. Raposinho PD, Correia JD, Alves S, Botelho MF, Santos AC, Santos I. A ^{99m}Tc(CO)$_3$-labeled pyrazolyl-α-melanocyte-stimulating hormone analog conjugate for melanoma targeting. *Nucl Med Biol.* 2008;35:91–99.
3. Guo H, Shenoy N, Gershman BM, Yang J, Sklar LA, Miao Y. Metastatic melanoma imaging with an ^{111}In-labeled lactam bridge-cyclized alpha-melanocyte-stimulating hormone peptide. *Nucl Med Biol.* 2009;36:267–276.
4. Guo H, Yang J, Gallazzi F, Prossnitz ER, Sklar LA, Miao Y. Effect of DOTA position on melanoma targeting and pharmacokinetic properties of ^{111}In-labeled lactam bridge-cyclized α-melanocyte stimulating hormone peptide. *Bioconjug Chem.* 2009;20:2162–2168.
5. Raposinho PD, Xavier C, Correia JD, Falcao S, Gomes P, Santos I. Melanoma targeting with alpha-melanocyte stimulating hormone analogs labeled with fac-[^{99m}Tc(CO)$_3$]$^+$: effect of cyclization on tumor-seeking properties. *J Biol Inorg Chem.* 2008;13:449–459.
6. Guo H, Yang J, Shenoy N, Miao Y. Gallium-67-labeled lactam bridge-cyclized alpha-melanocyte stimulating hormone peptide for primary and metastatic melanoma imaging. *Bioconjug Chem.* 2009;20:2356–2363.
7. Guo H, Yang J, Gallazzi F, Miao Y. Reduction of the ring size of radiolabeled lactam bridge-cyclized alpha-MSH peptide resulting in enhanced melanoma uptake. *J Nucl Med.* 2010;51:418–426.
8. Morais M, Oliveira BL, Correia JD, et al. Influence of the bifunctional chelator on the pharmacokinetic properties of ^{99m}Tc(CO)$_3$-labeled cyclic α-melanocyte stimulating hormone analog. *J Med Chem.* 2013;56:1961–1973.
9. Guo H, Yang J, Gallazzi F, Miao Y. Effects of the amino acid linkers on melanoma-targeting and pharmacokinetic properties of indium-111-labeled lactam bridge-cyclized α-MSH peptides. *J Nucl Med.* 2011;52:608–616.
10. Guo H, Miao Y. Cu-64-labeled lactam bridge-cyclized alpha-MSH peptides for PET imaging of melanoma. *Mol Pharm.* 2012;9:2322–2330.
11. Guo H, Gallazzi F, Miao Y. Ga-67-labeled lactam bridge-cyclized alpha-MSH peptides with enhanced melanoma uptake and reduced renal uptake. *Bioconjug Chem.* 2012;23:1341–1348.
12. Guo H, Gallazzi F, Miao Y. Design and evaluation of new Tc-99m-labeled lactam bridge-cyclized alpha-MSH peptides for melanoma imaging. *Mol Pharm.* 2013;10:1400–1408.
13. Hoffman TJ, Gali H, Smith CJ, et al. Novel series of ^{111}In-labeled bombesin analogs as potential radiopharmaceuticals for specific targeting of gastrin-releasing peptide receptors expressed on human prostate cancer cells. *J Nucl Med.* 2003;44: 823–831.
14. Garcia Garayoa E, Schweinsberg C, Maes V, et al. Influence of the molecular charge on the biodistribution of bombesin analogues labeled with the [^{99m}Tc(CO)$_3$]-core. *Bioconjug Chem.* 2008;19:2409–2416.
15. Fragogeorgi EA, Zikos C, Gourni E, et al. Spacer site modifications for the improvement of the *in vitro* and *in vivo* binding properties of ^{99m}Tc-N$_3$S-X-Bombesin[2-14] derivatives. *Bioconjug Chem.* 2009;20:856–867.
16. Garrison JC, Rold TL, Sieckman GL, et al. Evaluation of the pharmacokinetic effects of various linking group using the ^{111}In-DOTA-X-BBN(7-14)NH$_2$ structural paradigm in a prostate cancer model. *Bioconjug Chem.* 2008;19: 1803–1812.
17. Parry JJ, Kelly TS, Andrews R, Rogers BE. In vitro and in vivo evaluation of ^{64}Cu-labeled DOTA-Linker-Bombesin(7-14) analogues containing different amino acid linker moieties. *Bioconjug Chem.* 2007;18:1110–1117.
18. Liu S, He Z, Hsieh WY, Kim YS, Jiang Y. Impact of PKM linkers on biodistribution characteristics of the ^{99m}Tc-labeled cyclic RGDfK dimer. *Bioconjug Chem.* 2006;17:1499–1507.
19. Shi J, Wang L, Kim YS, et al. Improving tumor uptake and excretion kinetics of ^{99m}Tc-labeled cyclic arginine-glycine-aspartic (RGD) dimers with triglycine linkers. *J Med Chem.* 2008;51:7980–7990.
20. Wang L, Shi J, Kim YS, et al. Improving tumor-targeting capability and pharmacokinetics of ^{99m}Tc-labeled cyclic RGD dimers with PEG$_4$ linkers. *Mol Pharm.* 2009;6:231–245.
21. Shi J, Kim YS, Zhai S, Liu Z, Chen X, Liu S. Improving tumor uptake and pharmacokinetics of ^{64}Cu-labeled cyclic RGD peptide dimers with Gly$_3$ and PEG$_4$ linkers. *Bioconjug Chem.* 2009;20:750–759.
22. Miao Y Benwell K, Quinn TP. ^{99m}Tc and ^{111}In labeled alpha-melanocyte stimulating hormone peptides as imaging probes for primary and pulmonary metastatic melanoma detection. *J Nucl Med.* 2007;48:73–80.
23. Kasten BB, Ma X, Liu H, et al. Clickable, hydrophilic ligand for fac-[M^I(CO)$_3$]$^+$ (M = Re/^{99m}Tc) applied in an S-functionalized α-MSH peptide. *Bioconjug Chem.* 2014;25:579–592.
24. Jiang H, Kasten BB, Liu H, et al. Novel, cysteine-modified chelation strategy for the incorporation of [M^I(CO)$_3$]$^+$ (M = Re/^{99m}Tc) in an α-MSH peptide. *Bioconjug Chem.* 2012;23:2300–2312.